*Desalination and Water Treatment*
www.deswater.com

doi: 10.5004/dwt.2020.26035

194 (2020) 1–18
August

# Evaluation of desalinated seawater vs. filtered raw seawater for heap leach copper extraction on mountaintop mines in arid regions

Kenneth P. Goodboy[a], Thomas M. Missimer[b,*]

[a]*Triple Point Separations Technologies, LLC, 2695 Timberglen Drive, Wexford, PA 15090-7562, USA*
[b]*Emergent Technologies Institute, U.A. Whitaker College of Engineering, Florida Gulf Coast University, 16301 Innovation Lane, Fort Myers, Florida 33913, USA, email: tmissimer@fgcu.edu (T. Missimer)*

Received 13 April 2020; Accepted 28 April 2020

**ABSTRACT**

Numerous high-altitude copper mines occur in arid areas of northern Chile and Southern Peru in South America and other global regions. These mines require a water supply for on-site copper extraction, particularly those using the heap leach process. A common problem in determining the least costly option to obtain process water is a choice between pumping treated seawater or desalinated seawater (freshwater) from the coast to the mine site, commonly 600–4,900 m above sea level and 10–200 km inland from the shoreline. A detailed analysis of this problem was conducted to assess the key cost factors involved in water treatment, transport, and impacts on the heap leach process. The analysis showed that water treatment cost was 70% higher for desalted water, pump efficiency was 6.95% lower to transport seawater, in both cases, the transmission pipeline must be constructed with epoxy-coated steel, water reuse potential in the process was up to 70% greater using freshwater, the hydraulic conductivity of the heap material was 2.6% lower when using seawater, and the use of acid was more than 32 times greater when using seawater. Overall, the water type used showed little difference in cost when considering all factors. However, the use of seawater creates some additional operational factors in a greater volume of onsite salt and brine disposal and some potential environmental impacts. The use of freshwater may be preferred when considering the socio-political factor involving water supply to the local population and the residual value of the desalination facility.

*Keywords:* Seawater reverse osmosis desalination; Copper mining; Heap leach copper extraction; Economics of source water

## 1. Introduction

Mining in arid mountaintop environments can create some serious challenges that greatly impact the fundamental economics of copper production. Because of the transportation costs to move raw copper ore to lower altitudes for treatment, it is a common practice to use heap leach extraction at the mountaintop and transport only the enriched product down the mountain. The process of heap leach extraction of copper has become the preferred method of producing high-quality copper material at the mining sites [1–4]. While the heap leach extraction technology is well established, the fundamental issue has become the need to provide water for the process [5].

The mountaintop mines in northern Chile and southern Peru occur in very arid environments where there is either no source of freshwater at or near the mines or the lower altitude development of freshwater resources would conflict with the use of limited freshwater resources by the local population [6]. Therefore, the only viable source of water becomes desalted seawater or raw seawater that has to be pumped from sea level to altitudes primarily ranging between 2,500 and 4,300 m above sea level [7] (Fig. 1).

* Corresponding author.

1944-3994/1944-3986 

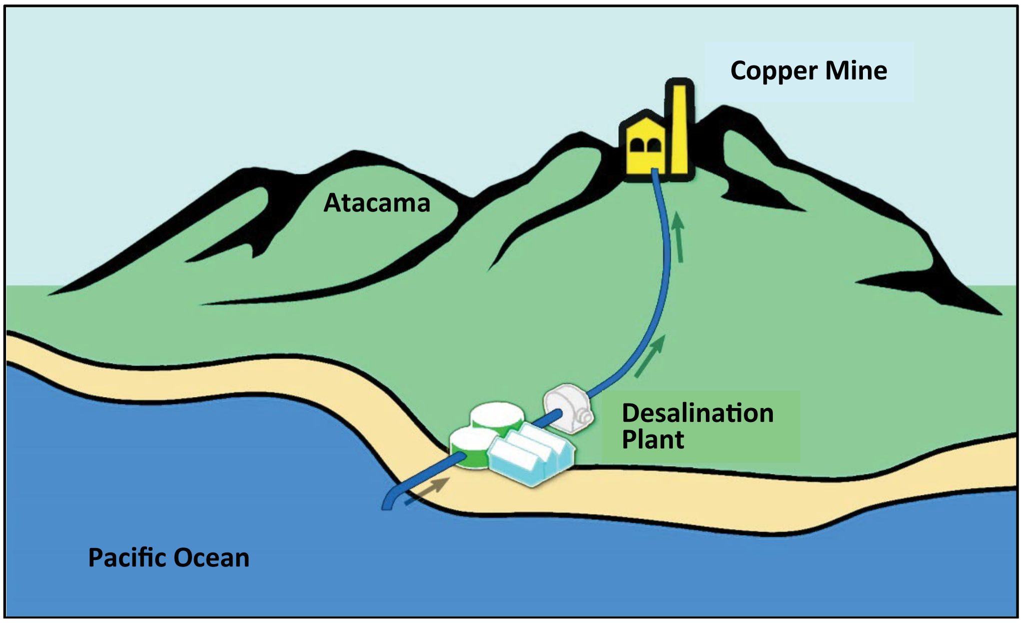


Fig. 1. Schematic diagram of the combined water source, transport pipeline, and mine.

Decision-makers at mining companies are faced with deciding whether to pump desalinated seawater up the mountain to the heap leach extraction facilities or to pump seawater to the site. Several important issues have to be considered: (1) the capital and operating costs of the seawater desalination facility; (2) the added cost of pumping seawater in lieu of freshwater to the necessary elevation based on the higher density and viscosity and the issue of greater corrosion of the pipeline; (3) the environmental effects of using seawater at the top of the drainage basin with potential impacts to lower altitude freshwater resources; and (4) the impacts of using seawater vs. freshwater in the heap leach process. This issue is a classic systems engineering design problem that is complex and requires considerable research with major economic and political ramifications. It is the purpose of this research to assess various engineering solutions concerning how to approach the problem with associated economic analyses.

## 2. Background

To evaluate this problem, it is necessary to assess several cost factors related to water treatment, water transport, impacts on the heap leach processes, and any created environmental issues. For evaluation purposes, a uniform water demand must be established, which in this case is set at about 75,708 $m^3$/d (about 20 MGD).

### *2.1. Seawater desalination*

Based on the required 75,708 $m^3$/d capacity to operate the heap leach process, a seawater reverse osmosis (SWRO) desalination plant would require an intake capacity of about 168,240 $m^3$/d (44 MGD) to produce the required product water with the assumption that the intake seawater has a total dissolved solids (TDS) concentration near 35,000 mg/L. The facility must be located close to the shoreline and would require the acquisition of new property or could be co-located with a shipping port associated with the transport of the product copper. The cost associated with the desalination plant includes capital costs for land acquisition and facility construction and the operating costs for desalting the water.

A major issue in remote coastal regions of Chile and Peru (and many other arid areas where copper can be mined) is the availability of electric power to operate the SWRO plant, the pumps to transport the water to the mine site, and the power required to operate the mine. In the case of the operation of a high-capacity SWRO plant, a new power generation plant would likely have to be constructed.

### *2.2. Transport of the water from the sea to the mining site*

Two options that require consideration include pumping desalinated water or pumping partially-treated seawater (removal of debris and particulate organics and sediments) to the mine site. Several fundamental issues that must be considered in the evaluation of the transport of either freshwater or seawater. The specific gravity difference between freshwater at 0.9986 and seawater at 1.025 will impact the pump design and the required horsepower to move the water to the high altitude. In addition, there may be a substantial difference in the pipeline design between one that can be used to transport freshwater vs. seawater based on corrosion potential.

### *2.3. Impacts of water quality on the heap leach process*

The heap leach process uses acidified water that is sprayed on top of the partially crushed rock that contains the copper ore. Typically, freshwater is used in the process. There is an additional cost for acidification when seawater is used instead of freshwater. Seawater commonly has a pH ranging from 8.00 to 8.45 and tends to be highly buffered with calcium bicarbonate, especially in warm, high-temperature areas with an arid climate (e.g., coastal Chile and Peru) because evaporative loses cause the upper part of the water column to become super-saturated with calcium bicarbonate. Therefore, to achieve the desired pH of the heap leach solution, additional acid will be required which is a significant cost due to the need to transport it via truck or pipeline to the mine site.

Another issue is that concerning the impact of the higher density seawater on the hydraulic conductivity of the crushed ore. Freshwater flows through the ore at the desired grain size at a predicted rate, but the density of seawater lowers the passage rate and could cause the crushed ore to have to be a larger mean grain diameter to operate efficiently. This issue could reduce the yield of copper per unit volume because of the reduced surface area of the grains in the heap.

### 2.4. Environmental impacts of using freshwater vs. seawater

The heap leach fluid is gathered from the collection area down-gradient from the piled, crushed rock, and pumped to the concentration plant for copper extraction (Fig. 2). The same occurs for both freshwater and seawater. However, the potential for recycling some of the freshwater back to the extraction process is generally higher compared to the use of seawater. In addition, the impacts of seawater vs. freshwater on the copper concentration and removal process must be carefully evaluated. Based on which type of water is used in the process, there may be less recycling of water and the amount of water requiring disposal may be larger for use of seawater. Since the mine sites contain little or no rainfall, lined evaporation basins can be used for water disposal with the salt harvested for disposal in some environmentally-friendly manner. If the salt must be transported a significant distance for disposal, the volume generated is an economic issue.

### 2.5. Socio-political issues related to choice of water source for copper mining

Mountaintop copper mining requires government permits to be issued, particularly in Peru and Chile, before mining activities can commence. The residents of these countries are quite sensitive to the environmental impacts of mining and any specific impacts to local water supplies. In most cases, there are no viable means of using sources of freshwater in competition with local farmers or residents. In locations where this has been attempted, permits were not issued and violence has occurred. The only long-term viable choices are to use either desalinated seawater or partially-treated seawater.

There is a potential advantage of developing a seawater desalination plant in the mining approval process wherein some side-stream from the SWRO plant could be used to supply some or all local residents with potable drinking water. Also, the SWRO plant may have a greater useful life-expectancy than the copper mine which leaves potential residual value to the operator and the local residents when the mine is closed. Also, the increased electric power generated to operate the SWRO plant could be diverted to local use to increase local grid reliability. These issues must be considered in the value-engineering of which water source to use, because of both the issue of providing greater security in the permitting process and the residual value when the facilities are left behind in the post-mining

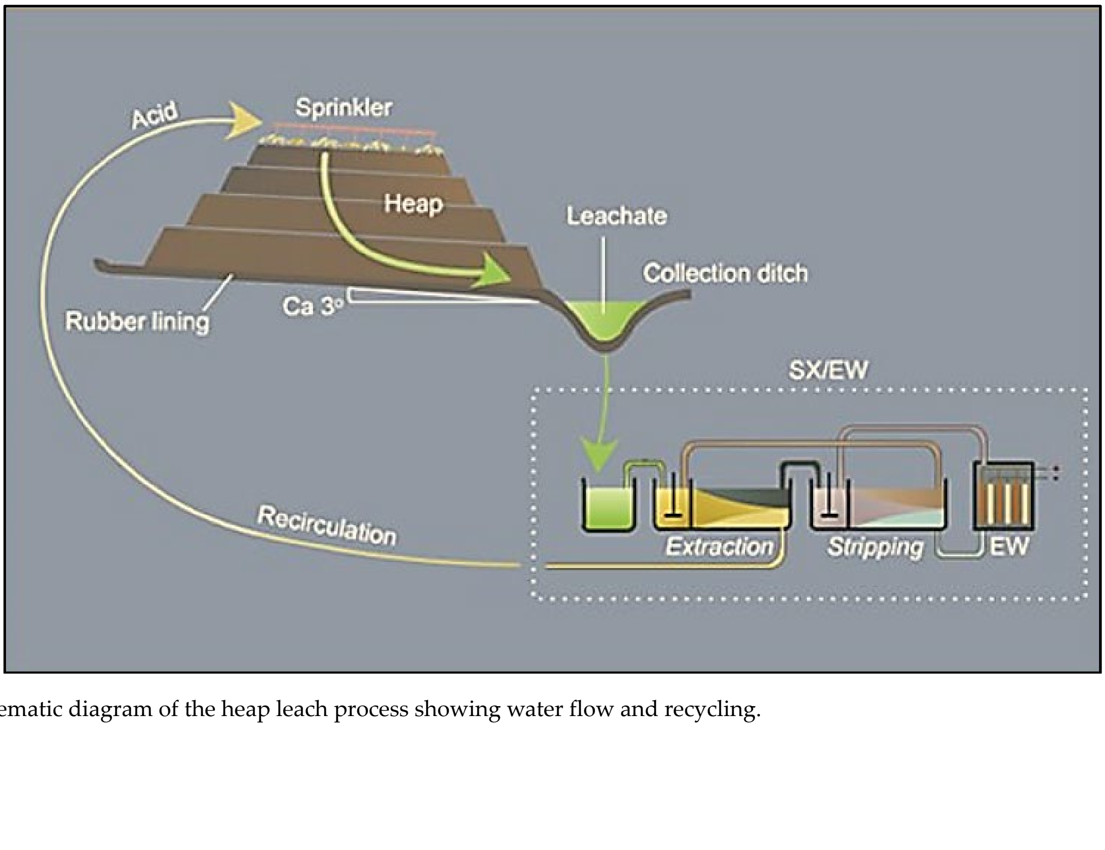


Fig. 2. Schematic diagram of the heap leach process showing water flow and recycling.

timeframe. There could be government-sponsored buyouts that could enhance local economic development.

## 3. Assessment of pipeline differences between SWRO permeate and treated seawater transport: water density and viscosity

### *3.1. Hydraulic analysis of pumping SWRO permeate vs. treated seawater*

#### *3.1.1. Economic optimum pipe diameter*

With the acute shortage of water in the mining regions of Northern Chile and Southern Peru, water pipelines normally start near the Pacific Ocean and traverse the Atacama Desert with lengths varying from 10 to 200 km to elevations of 600–4,900 m above sea level [8,9]. These pipelines are a huge capital expense (CapEx), and determining the economic optimum diameter, over the life of the project, is an important engineering calculation.

The economic optimum pipe diameter is a tradeoff between CapEx and the operating expense (OpEx). A larger pipe diameter, while keeping other pipe properties constant, will increase CapEx, while decreasing OpEx. The economic optimum diameter can be determined, over the life of the project, at the minimum of the yearly summation of CapEx and OpEx, as a function of inside pipe diameter, while keeping the other pipe properties constant. It should be mentioned that these mining pipelines can have from one to maybe five pumping stations traversing the Atacama Desert. The length and number of pipelines, the changes in elevation and terrain, and the water density and viscosity can all impact the design and location of the pumping stations. A methodology is presented to determine the economic optimum pipe diameter, with key assumptions, that lead to a cost comparison of SWRO permeate vs. treated seawater in internally coated carbon steel (C-steel) pipeline systems.

#### *3.1.2. Operating expense*

When a non-compressible fluid flows through a circular pipe of constant inside diameter, the total mechanical energy can be represented by Eq. (1), as taken from Genereaux [10], Peters and Timmerhaus [11–13], and Nolte [14], who have all presented methods for determining the economic optimum pipe diameter. For this analysis, Eq. (1) assumes the pipe is 100% full of liquid and therefore, no partial or mixed (gas + liquid) flow is occurring. Only the friction pressure drop needs to be included in Eq. (1), as the static head is not a function of the pipe diameter – only elevation [15]. Note that the equations use English values, which are later converted into metric results after calculation.

$$W = \frac{2f\,LV^2\left(1+J\right)}{gD} \tag{1}$$

where $W$ is the mechanical work added from pumps, ft–$lb_f/lb_m$; $f$ is the Fanning friction factor based on Eq. (2) Σ (friction), normally 0.0063 to 0.0118; $L$ is the length of pipe, ft; $V$ is the average linear velocity of the fluid, 3–10 ft/s is reasonable for new or coated C-steel pipe [16]; $J$ is the frictional loss due to fittings and bends, equivalent fractional loss in a straight pipe, approximately 0.35 or 35%, but should be determined [12]; $g = g_{45}$, the standard gravitational acceleration in a vacuum is exactly 9.80665 m/s$^2$; ≈32.17405 ft–$lb_m$/($s^2$·$lb_f$) at sea level and 45° latitude. It is a function of latitude (9.832 m$^2$/s at the poles, and 9.780 m/s$^2$ at the equator) and altitude [17]; $D$ is the inside diameter of the circular pipe, ft.

When the flow is turbulent, which requires the Reynolds number to be greater than approximately 2,000, the Fanning friction factor can be estimated from Eq. (2), when the C-steel pipe is smooth [12]. This requires the C-steel pipe to be new and/or evenly coated with a polymer inside for corrosion protection, and therefore provides a lower pressure drop or OpEx:

$$f = \frac{0.04}{\left(N_{\text{Re}}\right)^{0.16}} \tag{2}$$

where $N_{\text{Re}}$ is the Reynolds number = $\frac{DV\rho}{\mu}$; ρ is the fluid density, 61.940 to 65.943 lbs/ft$^3$, 0°C to 40°C, and 0 to 70 PSU (practical salinity unit); μ is the fluid viscosity, 0.6526 to 2.0723 cP, 0°C to 40°C, and 0 to 70 PSU.

Eq. (2) is similar to the expression developed for flow at $2{,}000 < N_{\text{Re}} < 100{,}000$ as shown in Eq. (3) [18], based on the time-averaged wall shear stress. The Blasius correlation produces a lower friction factor for the same $N_{\text{Re}}$. Eq. (2) is based on the critical shear stress, at the point of bursting in the wall layer process [19]. Both equations only apply to smooth pipe. At $N_{\text{Re}} = 2{,}000$, the two values are different by only 0.23% and increase to 10% difference at $N_{\text{Re}} = 5{,}622$.

$$f = \frac{0.079}{\left(N_{\text{Re}}\right)^{0.25}} \tag{3}$$

With the above conditions being met, and the internal pipe diameter ≥ 2.54 cm (1 inch), Eqs. (1) and (2) can be combined to yield Eq. (4), which can be used to determine the annual pumping cost or OpEx.

$$\text{OpEx} = \frac{0.273Q^{2.84}\rho^{0.84}\mu^{0.16}K\left(1+J\right)H}{D^{4.84}E} \tag{4}$$

where OpEx is the pumping cost, \$/y/ft; $Q$ is the flow rate, ft$^3$/s; $K$ is the cost of electrical energy, \$/kWh; $H$ is the hours of operation/y, normally 8,327.7 with 95% uptime and 365.25 d/y; $E$ is the overall efficiency of motor, variable frequency drive (VFD), and pump expressed as a decimal fraction. Large (>60 HP), enclosed premium motors are normally 95.0%–96.2% efficient at top loads [20,21]. VFD's are normally 94%–97% efficient depending on the load. Pump efficiency varies with pump type, size, and head. The motor, VFD, and pump efficiencies are multiplied times each other to obtain "*E*".

The efficiency of large NEMA premium enclosed pump motors is somewhat straightforward when controlled by VFD's near top loads [20]. But the efficiency of the respective pump is more complicated. Since water density and viscosity are the two variables that are being compared for SWRO permeate and treated seawater, a brief analysis is presented. In terms of water density, it is not a factor in hydraulic efficiency, as centrifugal pumps move a fixed volume that is a function of the revolutions per minute (rpm) of the respective impeller. But in terms of energy, increasing water density directly increases the pumping cost.

From research and field data, there is a revised procedure that corrects the pump performance as a function of viscosity, as pump curves are typically based on freshwater viscosity [22]. With a more viscous fluid, the pump efficiency decreases and is a function of the fluid viscosity, pump shaft rpm, water flow rate at the best efficiency point (BEP), and water head per stage at the BEP. The correction factor raises the viscosity term to the 0.5 power or square root. At 17.9°C, which is the average (13.1°C low in July, and 22.7°C high in March) annual surface seawater temperature in Taltal, Chile (Northern Chile) [23], the ratio of treated seawater viscosity at 34.5 PSU (1.1306 cP) to SWRO permeate viscosity at 0.25 PSU (1.0559 cP) is the ratio that needs to be considered. Therefore, the square root of 1.1306/1.0559 is 1.0348, or the seawater pump efficiency needs to be downgraded 3.48% keeping all other variables constant [24]. The pump efficiency is in the denominator of Eq. (4), and the reciprocal is required, which yields 0.96640 and therefore increases the cost of pumping treated seawater or a more viscous fluid.

### 3.1.3. Capital expense

For most pipe types, a log-log plot of the purchased price of the pipe, per linear meter (foot), vs. pipe inside diameter, will yield a straight line as shown in Fig. 3. The pressure rating or wall thickness of the pipe must be constant along with the yield strength of the C-steel. The pipe cost data in Fig. 3 are real, but have not been updated, and are only used for illustrative purposes. Pipe costs are a function of the C-steel alloy type, inside diameter, wall thickness, tensile strength, and coatings, etc.

A pipe under load exhibits both longitudinal and hoop stresses. Longitudinal stress is tensile stress, which tends to stretch the pipe axially and typically produces a circumferential fracture. While hoop stress is a “ballooning” or radial expansion and the typical failure is a lengthwise split of the pipe. Eqs. (5) and (6) show that longitudinal stress is twice hoop stress, and therefore longitudinal stress is normally the primary limiting design stress.

$$\text{Longitudinal stress} = \frac{P \times \text{OD}}{2 \times t} \tag{5}$$

$$\text{Hoop stress} = \frac{P \times \text{OD}}{4 \times t} \tag{6}$$

where stress is in psia; $P$ is the maximum operating pressure, psia; OD is the pipe outside diameter, inches; $t$ is the wall thickness, inches.

The required tensile strength of C-steel needs to be carefully evaluated, as the cost of seamless API 5L x65 vs. x46 pipe, can be a factor of 2.47 times more expensive

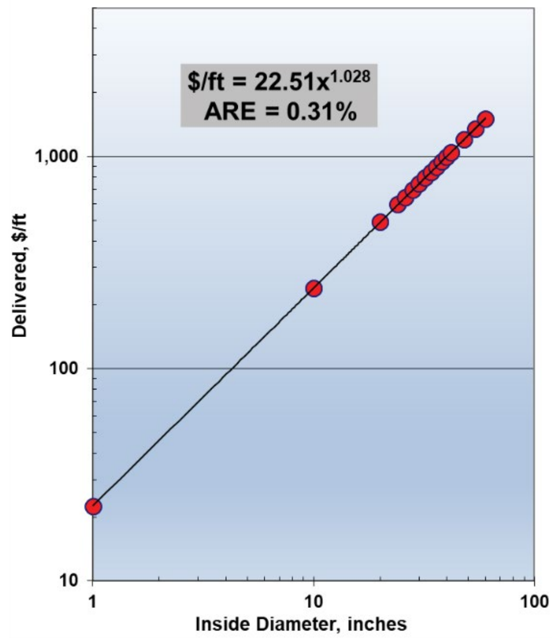


Fig. 3. Seamless API 5L x60 PSL2, ½″ wall thickness.

[25]. The required wall thickness is inversely related to the tensile strength of the C-steel. Therefore, API 5L x65 vs. x46 tensile strength pipe could have a wall thickness 65/46 = 1.41 times thinner, but there are other considerations, as will be shown later. Over the last 40 y, the optimum velocity in pipelines has decreased [26] and therefore must be updated for any project, as prices can change at any time.

A log–log plot yields the generic Eq. (7) for the purchased cost of pipe, which should include the freight for delivery to the construction site.

$$\text{CapEx} = XD^n \tag{7}$$

where CapEx is the purchased cost of delivered new pipe, $/ft; $X$ is the purchased cost of pipe/ft if the pipe diameter is 1 inch, 22.51 $/ft in the example; $n$ is the constant with the value dependent on the pipe type, 1.028 in the example, but can range up to 1.50 for new C-steel pipe ≥ 1 inch [12,26].

Using conventional least-squares regression of the pipe costs generates an $R^2$ value of 99.995% with an absolute average error (ARE) of 1.96%; therefore, the assumption for Eq. (7) is valid for this application. The actual ARE of Fig. 3 is 0.31%, as the coefficients were optimized to minimize the ARE. Therefore, the annual cost for the installed piping may be expressed as Eq. (8).

$$\text{CapEx} = (1 + F)XD^nM \tag{8}$$

where CapEx is the purchased cost for delivered pipe, $/y/ft (converted to metric); $F$ is the ratio of total costs for fittings and installation, to purchase cost of delivered new pipe, normally in the range of 1.4, but should be determined [12]; $M$ is the annual maintenance, expressed as a fraction of initial cost for completely installed pipe, approximately 0.20 or 20%, but should be determined [12] and will be much lower for a pipe that is coated on the inside and outside.

When the CapEx and OpEx equations are combined, taking the first derivative, and setting the equation to zero, and accounting for the units of the variables, the economic optimum diameter can be determined using Eq. (9) [12].

$$D = \left[ \frac{1.32Q^{2.84}\rho^{0.84}\mu^{0.16}K(1+J)H}{n(1+F)X\,E\,M} \right]^{\frac{1}{4.84+n}} \quad (9)$$

Eq. (9) does not include the cost of capital, pump stations, taxes, nor the time value of money, and these values can be included in the determination of the economic optimum diameter [12], but are not necessary for comparing SWRO permeate to treated seawater. The variables that are most important in Eq. (9) are those with the highest exponent, that is, flow rate, and then the linear variables.

Eq. (9) can be easily compared for SWRO permeate and treated seawater, as the two terms that vary with the water type are the fluid density and viscosity. Both SWRO permeate and treated seawater is very corrosive and it is the authors' opinion that a non-coated pipeline should not be used based on the case histories and research that is herein presented. Therefore, the maintenance costs are assumed to be equal, but with the key assumption that raw seawater is filtered extremely well with a combination of dissolved air floatation (DAF) and ultrafiltration (UF) systems or seawater intake wells. One of these filtration designs would also be installed in a SWRO facility.

Both fluid density and viscosity are a function of temperature and salinity. The average annual surface seawater temperature in Taltal, Chile is approximately 17.9°C, as previously stated, and with seasonal variations, it decreases 1.5°C–4.0°C at 20 m depth. Greater seawater intake depths will normally result in even lower temperatures, but the highest temperate is desired to maximize the membrane flux.

The average worldwide surface seawater salinity is 35 PSU and the seawater salinity is 34.5 PSU in Taltal, Chile as the Chile/Peru sea-current comes from the south, where Antarctic Circumpolar ice water partially dilutes the seawater [27]. Table 1 shows that although there are definitely differences in the density and viscosity of (1) 0.25 PSU SWRO permeate, (2) treated seawater at 34.5 PSU, and (3) SWRO brine concentrate at 70 PSU, when the two variables are taken to an exponent of less than one, and multiplied together, as shown in the $\rho^{0.84}\mu^{0.16}$ column of Table 1, the difference greatly decreases.

When the $\rho^{0.84}\mu^{0.16}$ ratio of 34.5 PSU treated seawater to 0.25 PSU SWRO is calculated, the average result is 1.0336% or 3.36% higher operating costs. But when the salt content of the 70 PSU brine concentrate is considered, the average change in operating costs increases to 7.17%. The 70 PSU brine concentrate is primarily used to show the trend, as it is normally properly disposed of at the SWRO plant into the Pacific Ocean, but it should be pointed out that seawater that was partly recirculated at the Las Luces, Chilean mine had a 46 PSU after 15 y due to evaporation [28].

The 3.36% increase in treated seawater pumping costs must be increased by the decreased pump efficiency of pumping treated seawater vs. SWRO permeate, which was previously determined as 0.96640. Therefore, the total increase, in pumping treated seawater vs. SWRO permeate, amounts to 1.0336/0.96640 = 1.0695 or approximately 6.95% in northern Chile and Southern Peru for coated C-steel pipelines.

This increase in pumping treated seawater vs. SWRO permeate is not to be taken as an absolute number. The preferred pump manufacture should be consulted as to whether or not the viscosity adjustment is totally applicable to their particular pump data, because as previously mentioned, four variables are involved in the performance factor term [22]. The purpose of this discussion is to inform the reader of the pump viscosity issue for further investigation for their particular project.

## 4. Corrosion considerations of SWRO permeate and seawater

### 4.1. Introduction

SWRO permeate and seawater are both corrosive to unprotected C-steel but at different rates. If a corrosion

Table 1
Comparison of SWRO permeate, treated seawater, and brine concentrate

| Water type | °C | Density, g/cc | Viscosity, cP | $\rho^{0.84}\mu^{0.16}$ | Ratio water type/ SWRO $\rho^{0.84}\mu^{0.16}$ |
|---|---|---|---|---|---|
| | 13.1 | 0.9992 | 1.1981 | 1.0286 | |
| 0.25 PSU SWRO permeate | 17.9 | 0.9984 | 1.0559 | 1.0074 | |
| | 22.7 | 0.9974 | 0.9390 | 0.9878 | |
| | 13.1 | 1.0260 | 1.2806 | 1.0630 | 1.0334 |
| 34.5 PSU treated seawater | 17.9 | 1.0250 | 1.1306 | 1.0412 | 1.0336 |
| | 22.7 | 1.0238 | 1.0071 | 1.0211 | 1.0337 |
| | 13.1 | 1.0539 | 1.3955 | 1.1023 | 1.0716 |
| 70 PSU brine concentrate | 17.9 | 1.0527 | 1.2328 | 1.0796 | 1.0717 |
| | 22.7 | 1.0512 | 1.0989 | 1.0587 | 1.0717 |

inhibitor were to be added to the respective water, this would decrease the effectiveness of the water in the heap leach process by requiring more acid to be used and would likely still have sufficient corrosivity to require a coated pipeline to be used. In both SWRO permeate and seawater, the same corrosion mechanisms apply, but with seawater, there are additional corrosion processes. The average worldwide surface seawater salinity is 35 PSU and equals 35.16504 ± 0.007 g/kg, which is approximately 3.5 weight %, consisting of 15 significant solutes [29]. With 34.5 PSU seawater in Northern Chile and Southern Peru as the source, SWRO permeate has low TDS at ≈250 mg/L with reasonably-aged SWRO membranes. This TDS in the SWRO permeate results in a chloride concentration of approximately 140 mg/L as shown in Table 2, which is less than the maximum chloride that can be tolerated for drinking water before it starts to taste salty at 250 mg/L chloride [30]. But SWRO permeate increases to ≈500 mg/L TDS when the seawater salinity increases to 45 PSU in other parts of the world [31]. The SWRO permeate TDS is a function of the feed PSU and temperature, membrane type(s) and age, number of elements per vessel, recovery, flux, and number of stages/passes. Some SWRO systems also have an adjacent power plant that requires higher purity permeate, and therefore it will have an additional pass or treatment process like electrodeionization. For agricultural applications, part of the flow will go to a second pass for further boron removal.

#### 4.1.1. C-steel

When just considering C-steel, corrosion is a function of the C-steel chemistry, uniformity, surface hardness, and surface roughness. Intergranular corrosion is a water cation/anion, or $O_2$ attack on the grain boundaries of C-steel, primarily due to impurities in the C-steel. These grain boundaries can corrode faster than the bulk of C-steel.

#### 4.1.2. Dissolved $O_2$, $Cl^-$, $SO_4^{-2}$, bioactivity, and erosion

At atmospheric pressure and 17.9°C for Taltal, Chile annual surface seawater temperature, SWRO permeate, at 250 mg/L TDS, contains 9.47 ± 0.001 mg/L of dissolved oxygen (DO) [32], as shown in Table 2. This DO concentration will attack unprotected C-steel over time, especially with chloride ions present. The DO content of water decreases with increasing temperature, lower total pressure, and increasing TDS. SWRO permeate is an unbuffered water, in that addition of small concentrations of ions can easily change the pH; a case in point is the carbon dioxide ($CO_2$) content, which can also be highly corrosive.

Table 2
Typical 34.5 PSU surface seawater and SWRO permeate at 17.9°C and 1 atm

| Water source | $O_2$, mg/L | TDS, mg/L | $Cl^-$, mg/L | $SO_4^{-2}$, mg/L |
|---|---|---|---|---|
| SWRO permeate | 9.47 | 250 | 140 | 6 |
| Natural seawater | 7.71 | 34,500 | 19,400 | 2,700 |

On the other hand, seawater is corrosive for the same reasons as SWRO permeate with several additional mechanisms: (1) at 34.5 PSU, 17.9°C and atmospheric pressure, seawater has 7.71 ± 0.001 mg/L of DO [32], assuming no biological activity, (2) the chloride content is high at about 19,400 mg/L [29], which can cause severe pitting, (3) the sulfate content is high at about 2,700 mg/L [29], which can cause hydrogen sulfide ($H_2S$) formation from sulfate-reducing bacteria (SRB) and $H_2S$ is very corrosive, (4) seawater can have various types and degrees of bioactivity, which can cause severe biofouling [33], and (5) seawater can contain grit (sand, seashell particulates, etc.) which can cause pipeline erosion and pump damage (should be removed in pretreatment processes).

#### 4.1.3. Temperature and pH

In water service with C-steel pipelines, temperature can increase the corrosion rate approximately 2%–4% per °C [34,35] depending on the DO content and velocity. Water pH is also a major corrosion variable, which is dependent on the temperature and the ions and concentrations that are present. Depending on the temperature, in acidic solutions at a pH between 4 and 5, $H_2$ evolution tends to eliminate the protective film formation, so that C-steel continues to corrode, and exponentially at an even lower pH [36]. In alkaline solutions with pH > 10, the formation of protective films greatly reduces the corrosion rate at seawater temperatures, but in power plant boilers, which are often associated with SWRO plants, at high temperatures, the corrosion chemistry is totally different.

#### 4.1.4. Velocity

As the velocity or Reynolds number increases, corrosion generally increases due to the higher mass transfer rate of DO, $Cl^-$, and $SO_4^{-2}$ [34]. Furthermore, the pipeline can have flow-assisted or flow-accelerated corrosion when a protective layer (oxide, etc.) on the C-steel is removed by the water velocity. Velocity is also a key variable in erosion from particulates in seawater. Therefore, C-steel corrosion, in various types of water, is a costly process and very a complicated topic. The following sections will present case histories and laboratory research on SWRO permeate and treated seawater in C-steel and coated C-steel pipelines.

It should be noted that corrosion studies seldom produce invariable test results, for the reasons stated above, and thus there is a requirement for two or more duplicate samples. Normally the test results are somewhat random,

Table 3
Maximum pitting after 365 d

| Test | Seawater and 365 d maximum pitting | Deposits applied | Nitrate | Depth, mm |
|---|---|---|---|---|
| 1 | Natural | | | 0.159 |
| 4 | Filtered and UV treated | | | 0.361 |
| 2 | Natural | | | 0.393 |
| 3 | Natural | | | 0.421 |

in that the whole test piece is not uniformly corroded, as the test piece itself is not absolutely the same throughout in structure or composition. Therefore, corrosion testing is extremely useful, and the more samples tested, the better the conclusion. Furthermore, it is highly recommended for any project that corrosion experiments be conducted on a representative, including coated, test specimens under the anticipated extremes and most probable operating conditions over the anticipated life of the project.

### *4.2. NACE®*

NACE International, with headquarters in Houston, Texas, is a non-profit professional organization for the control of corrosion. As a prelude to the following sections, NACE states, for the oil and gas industry, that corrosion in seawater injection systems is primarily caused by the presence of DO, bacteria, or concentration cells from solids in seawater.

In addition to mechanical removal of DO to 20 ppb (parts per billion), ammonium or sodium bisulfite should be added to the seawater in liquid form. Ammonium bisulfite is more concentrated, due to its higher solubility in water, and in this form, is a little more resistant to oxidation by the atmosphere. Care should be taken to not add too much excessive antioxidant, as in some systems it can lead to an increase in the corrosion rate [37].

Solids in seawater should be removed because corrosion increases under sediment or bacterial deposits. Seawater can contain both aerobic and anaerobic bacteria and recent research identified 23 different bacteria species in seawater at 5 desalination sites in Saudi Arabia, and the bacteria can be different in worldwide locations [33]. So, an oxidizing biocide like NaOCl or $ClO_2$ must be used. However, some seawater bacteria are resistant to oxidizing agents and seawater contains about 2,700 mg/L of $SO_4^{-2}$ [29]. Therefore, organic biocides need to be also carefully considered, as some interfere with the bisulfite for DO maintenance. The specification also states that C-steel piping should not be used with raw seawater that contains DO, and furthermore, there is a trend to use duplex stainless steels for seawater injection to reduce corrosion [37]. A thinner duplex stainless steel, vs. C-steel, can normally withstand the same pressure and save valuable weight for offshore platforms.

## 5. Seawater in C-steel pipelines

### *5.1. Kuwait*

Seawater injection is an effective method of increasing oil recovery, but the degree of success is dependent on the quality of the injection seawater and its compatibility with the reservoir. Kuwait Oil Company has a 914 mm (36 in) seawater pipeline that is 48 km long, and it was constructed of API 5L-B C-steel. At the time of the article, the pipeline had been operating for 9 y. The wall thickness was 10.3 mm for the first 41.6 km and 8.7 mm for the remainder of the pipeline, with a maximum operating pressure of 2.09 MPa (303 psig). The pipeline transports seawater that has been deaereated and treated with scale and corrosion inhibitors, and biocides. Seawater bacteria are difficult to remove because they are typically located beneath the biomass products [38]. Therefore, the scale and corrosion products, which accumulate over time, need to be periodically removed.

Intelligent pigs with a high-resolution magnetic flux leakage detection technique were used to detect and measure pipe wall defects that occur from corrosion and welding. The pipeline had a minimum radius at bends of 3 times the diameter. The types of corrosion that the intelligent pig determined were: (1) general, (2) pitting, (3) circumferential grooving (CIGR), and (4) circumferential slotting (CISL). Over a 3.30 y period, 30,068 kg of solids were removed from the pipeline. The intelligent pigs detected severe pitting from 30 km to the end of the pipeline, with 16 locations having a pit depth of 20% of the wall thickness. Although pitting was found at all circumference locations, the majority were located at the 4 to 8o'clock positions, which is the bottom section of the pipeline. Outlet sections were also prone to the accumulation of deposits that had bacterial corrosion underneath. Furthermore, from 30 km to the end of the pipeline, there was a high amount of CIGR and CISL [38].

Pigging requires downtime, and the mining industry in Northern Chile and Southern Peru today typically requires 95% uptime, due to the huge capital investment. There is a 508 mm (20 inches) diameter, 941 km long pipeline that transports natural gas from Coronel Cornejo, Salta, Argentina (Northwest) to the port of Mejillones, Chile [39]. The pipeline crosses over the Atacama Desert and reaches an elevation of 5,000 m above sea level. This pipeline has five pig launchers and was completed in 1999; it is not a water pipeline but demonstrates that pipeline pigging is used in Chile.

### *5.2. North Sea and Australia*

In the offshore oil and gas industry, seawater injection is also often used to increase the oilfield yield. Typically, uncoated API 5L-B C-steel pipelines are used, as in the Kuwait case, and are often many kilometers long at very high pressures. Usually, the seawater is mechanically deaerated to 20 ppb DO or less and treated with $NaHSO_3$ to maintain DO free seawater. The raw seawater is usually filtered with Amiad® 80 μm filters, and then in stages with 10, 5, and 1 μm Pall® FSI™ bag filters to remove sand, seashell particulates, and large organic matter. The final treatment is ultraviolet (UV) radiation at 254 nm wavelength to kill bacteria. This seawater processing will be herein referred to as "treated" seawater. Pigging is not always used to periodically remove solids from the offshore pipelines. Furthermore, $Ca(NO_3)_2$ or $NaNO_3$ is typically added to suppress $H_2S$ formation from seawater bacteria [40]. As in the Kuwait case, corrosion is usually worse at the 6 o'clock position and it is referred to as channeling corrosion.

In 1997, 23 seawater injection systems were inspected in the North Sea and it was found that 39% of them had failed due to channeling corrosion. Some of these pipelines were only in service 4–15 y with an expected service life of 20–25 y. The main causes of corrosion were found to be: (1) channeling corrosion associated with the use of nitrate, (2) under deposit corrosion with low seawater velocity, (3) microbiologically influenced corrosion (MIC), and (4) pitting corrosion. These four corrosion mechanisms are all significant for C-steel seawater injection pipelines. Furthermore, MnS inclusions, which can be present in C-steels, are believed to sustain the corrosion process [40]. In seawater, the critical nutrient in MIC is dissolved inorganic nitrogen, usually a nitrate.

The corrosion products typically include $Fe_3O_4$ (magnetite) at ≈48%, $CaCO_3$ (calcium carbonate) ≈26%, and sea sand ≈26%. Recent research at the University of Newcastle in Australia, in controlled laboratory conditions, investigated the following four test waters at 30°C, using 90 mm pipe sections, with 127.47 g of deposits as indicated in Table 3 [40].

- Natural seawater;
- Natural seawater with deposits applied;
- Natural seawater with deposits applied and nitrates;
- Filtered and UV treated seawater with deposits applied;

The conclusions that were obtained from the research were:

- Pitting was worse when there were deposits present and still occurred even at very low DO concentrations due to chloride presence.
- Nitrate addition, with deposits, created the deepest pit of 0.421 mm after 1 y.
- There were no microorganisms in the corrosion products when the seawater was UV irradiated and had the lowest pit depth when deposits were present.
- It is interesting to note that without deposits, natural seawater was the least fouling, which helps explain one of the most important corrosion conditions, that is, deposits. It is the opinion of the authors that pigging would decrease pitting, but not eliminate it and "continuous" pigging is not practical.

Furthermore, cartridge filtration has been shown to not be especially effective, and UF or seawater intake wells were required to remove most of the bacteria [33].

## 6. SWRO permeate in C-steel pipelines

### *6.1. Seawater and SWRO permeate pH*

Surface seawater typically has a pH between 8.00 and 8.45 with an average current worldwide value of ≈8.10, with the higher pH values in the northern hemisphere [41–43]. In dilute solutions, the definition of pH is the measurement of the $H^+$ ion concentration at 25°C. However, activity coefficients are not accurately estimated at salinities greater than ≈5 PSU for pH measurements via the conventional definition. A better pH definition is the seawater scale (SWS) pH that is shown in Eq. (10) [42].

$$pH_{SWS} \approx -\log_{10}\left\{\left[H^+\right]+\left[HSO4^-\right]+\left[HF\right]\right\} \tag{10}$$

where [] is the molinity in seawater, $mol/kg_{soln}$.

Furthermore, in conventional pH probes, $F^-$ and $Br^-$ in seawater interfere with $Ag^+$ in silver-silver chloride half cells. Nevertheless, there are multiple methods to obtain a pH value in seawater. For example, spectroscopic pH methods can measure seawater to ±0.0004 pH units [42].

Ocean pH has decreased in recent times, as more and more $CO_2$ is adsorbed [43,44]. The pH of the ocean has decreased by 0.1 units since the beginning of the industrial era with a corresponding 26% ($10^{0.1}$ = 1.2589) increase in hydrogen ion concentration [43]. Seawater is not acidic, but the high chloride content in combination with DO is normally a major corrosion issue. Furthermore, SWRO plants usually use spiral-wound membranes and therefore require pretreatment to remove as much suspended solids as possible. The better the pretreatment, the less downtime will be required for SWRO membrane cleaning, and also a higher operating flux ($L/m^2/h$ or $gal/d/ft^2$) can be utilized.

Today, more and more SWRO plants are using UF membrane filtration at 0.01 to 0.1 μm (0.00001 to 0.0001 mm) equivalent pore diameter, preceded by DAF for algal blooms cell removal, or seawater intake wells [33,45], as the preferred pretreatment technologies. Algal blooms are occurring more frequently and are more severe with increasing global ocean temperatures [46,47]. Algal blooms or harmful algal blooms (HAB's) occur on average 1.2 times/y, based on almost four decades of data, for Moreno Bay, Chile (near Antofagasta), and the surrounding tidal waters. The HAB's have generated very corrosive $H_2S$ from SRB's reacting with seawater sulfate [48].

SWRO plants do not use C-steel in any part of the process pipework; they normally use super duplex stainless steels which contain high concentrations of Ni, Cr, and Mo with traces of other elements such as N, and low C for weldability, that is, AL-6XN®, 254 SMO®, SAF 2507®, and Zeron-100® for example. The steel pitting resistance equivalent number (PREN) is shown in Eq. (11), and there is a high correlation between an increasing PREN number with decreasing pitting and crevice corrosions. A PREN number of >40 is normally required for SWRO plants.

$$PREN = \%Cr + 3.3(\%Mo + 0.5\%W) + 16\%N \tag{11}$$

where % is the weight percent of the element.

Furthermore, SWRO plants normally operate at pressures of 6.89 to 8.27 MPa (1,000 to 1,200 psia) and sometimes higher, depending on the osmotic pressure of the seawater, which is a function of the ion concentrations and temperature. The high pressures require even more attention to corrosion issues so that the plant may last 25 y or more.

As stated previously, SWRO permeate is an unbuffered water and $CO_2$ can lower the pH to approximately 5.90 ± 0.70, depending on the SWRO permeate composition, and especially the carbonic acid concentration. This is clearly in the acidic pH region and would be very corrosive to unprotected C-steel. During SWRO post-treatment, $CaHCO_3$ (calcium bicarbonate) is normally added to SWRO permeate to raise the pH to the range of approximately 8.20 ± 0.10 with hardness added to make the potable water healthier to drink and decrease corrosion potential.

### *6.2. Saudi Arabia*

Historically, desalinated seawater, from distillation or SWRO, in Saudi Arabia is pumped through either cement lined or polymer-coated pipelines. Table 4 lists the major materials that have been used in the construction of pipelines

Table 4
Chemical composition of alloys tested

| # | Steel alloy | AISI type | UNS No. | Maximum %C | %Cr | %Ni |
|---|---|---|---|---|---|---|
| 1 | C-steel | CS-1018 | J2503 | 0.25 | 0.5 max | 0.5 max |
| 2 | Electroless Ni plated C-steel | 1018ENP | – | – | – | – |
| 3 | Austenitic stainless steel | 304SS | S30400 | 0.08 | 18–20 | 8–12 |
| 4 | Martensitic Cr stainless steel | 410SS | S41000 | 0.15 | 11.5–13.5 | – |
| 5 | Martensitic Cr stainless steel | 420SS | S42000 | 0.35–0.45 | 12–14 | 0.5 max |
| 6 | Martensitic Cr stainless steel | 431SS | S43100 | 0.2 | 15–17 | 1.25–2.5 |

C-steel also contains 0.3% max Cu, and 0.6% max Si; electroless coating is 30 μm.

in Saudi Arabia, which includes pumps and valves. All of these materials were used in a 450 km long cement-lined SWRO permeate pipeline [31].

The alloys in Table 4 were evaluated at 250 and 350 mg/L dissolved chloride at a pH of 8.50 and a temperature range of 35°C to 50°C with deaerated water in a laboratory. Also, 2 and 15 ppm of $Zn(PO)_3$ (zinc hexametaphosphate, ZHMP) was tested as a corrosion inhibitor. A dynamic loop test was carried out per ASTM G31-72 (1990). For brevity purposes, not all of the test data are presented in Table 5. The following corrosion rate definitions apply in mills per year (mpy): low < 1, moderate 1.0–4.9, high 5.0–10, and severe >10 [49].

In summary, high chromium steels (>15% Cr) appear to provide good resistance to SWRO permeate; whereas lower chromium steels exhibit generally poor resistance under the test conditions [31]. Under dynamic (flow) conditions, C-steel corroded significantly, and ZHMP decreased the corrosion rate, but it was still in the severe range as previously defined [31].

The Kuwait, North Sea, Australian, and Saudi Arabian case histories and laboratory experiments serve to show that using non-coated C-steel for a pipeline has numerous corrosion issues, even with SWRO permeate, and especially with seawater. Use of non-coated C-steel, in a pipeline to a mine from the shore, for a mine with a useful life beyond 10 y, is economically not probable.

## 7. Pipeline coatings and installation economic alternatives

Even with the use of DAF/UF or seawater wells to produce filtered seawater with biocides, antiscalants, and corrosion inhibitors for transport in a C-steel pipeline will still require a large amount of maintenance, and the useful life of the pipeline will be shortened. Since pipelines for the mining industry must last approximately 25 y or longer with 95% uptime, the use of uncoated C-steel does not appear practical based on oil and gas industry experience and research.

It has previously been presented that the economics for a Chilean pipeline favor SWRO permeate, with a fusion bonded epoxy (FBE) coated pipeline, vs. an uncoated C-steel pipeline for seawater, as a corrosion allowance must be added in the latter case [50]. In that study, a conservative general corrosion value of 0.09 mm/y (3.5 mpy, moderate) was used, which over 25 y amounts to 2.25 mm of additional wall thickness. The problem with general corrosion allowances is that they assume a uniform corrosion rate along the entire pipeline, which is seldom if ever the case. Pitting would most likely cause a failure first vs. uniform general corrosion. Nevertheless, the power cost was 18.2% higher over the life of the project, due to the increase in pressure drop of an uncoated C-steel pipeline [50]. Chemical costs (additional acid for the heap leach process) for seawater were not considered and would make SWRO permeate even more favorable. In addition, the issue of reduced

Table 5
Corrosion test results on various steel alloys, mpy

| # | Test conditions | Jet impingement | | | Dynamic loop | | | | Crevice | | |
|---|---|---|---|---|---|---|---|---|---|---|---|
| 1 | Chloride, mg/L | 350 | 350 | 350 | 350 | 350 | 350 | 250 | 350 | 250 | 350 |
| 2 | Temperature, °C | 35 | 50 | 35 | 40 ± 3 | | | 45 | | | |
| 3 | Velocity, m/s | 10 | 10 | 10 | 4 | 4 | 4 | | Stagnant | | |
| 4 | ZHMP, mg/L | 0 | 0 | 2 | 0 | 2 | 15 | 0 | 2 | | |
| | Steel alloy | | | | | | | | | | |
| 1 | CS-1018 | 28 | 29 | 6.0 | 114.1 | 37.9 | 22.2 | 17.2 | 16.5 | 4.2 | 5.0 |
| 2 | Ni plated C-steel | 1.1 | 1.3 | 1.0 | 2.3 | 1.7 | 0.8 | 2.3 | 3.1 | 0.5 | 1.0 |
| 3 | 304SS | 0 | 0 | 0 | 0 | 0 | 0 | 0 | 0 | 0 | 0 |
| 4 | 410SS | 4.8 | 5.3 | 0.4 | 3.4 | 2.6 | 2.6 | 19.5 | 2.1 | 0.5 | 0.8 |
| 5 | 420SS | 1.1 | 1.7 | 0.1 | 0 | 0 | 0 | 0.35 | 1.25 | 0.8 | 0.5 |
| 6 | 431SS | 0 | 0 | 0 | 0 | 0 | 0 | 1.0 | 0 | 0 | 0 |

intrinsic permeability, caused by the denser seawater, was also not considered with implications of reduced copper yield from the crushed ore during leaching. Therefore, the results of this study are somewhat conservative and still, the SWRO permeate with an FBE coated pipeline was more economical than an uncoated C-steel pipeline with partially-treated seawater.

### *7.1. DO removal*

Desalinated seawater is also corrosive and a DO removal system would have to be installed for an uncoated C-steel pipeline. If a well intake system is used instead of surface seawater, the SWRO permeate could contain some $H_2S$ that would also have to be removed. Chloride accelerates the DO corrosion rate on C-steel [51]. Today there are hydrophobic membrane systems that will more efficiently reduce DO in water, but the cost of the system is exponential with lower and lower DO concentrations as shown in Fig. 4. The requirement of 20 ppb is not easy to meet via mechanical means, as it requires exponentially more membranes the lower the required DO target, but DO removal is not required in a properly coated C-steel pipeline.

### *7.2. Pipeline coatings and liners*

Previously, anticipated pipeline diameters for mining in Chile was stated as 610 to 1,523 mm (24 to 60 inches) [8], but on recent projects, the range has been narrowed to 610 to 1,067 mm (24 to 42 inches) as shown in Table 6 [52–54]. BHP Billiton, on the new Escondida expansion, chose dual 1,067 mm (42 inches) SWRO pipelines, which

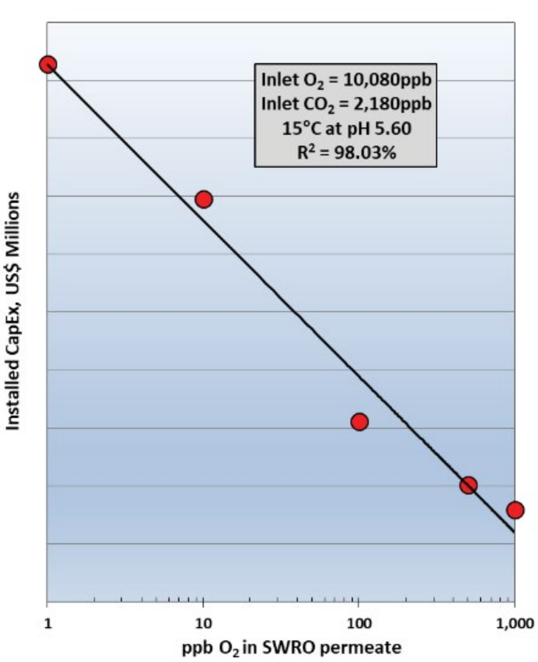


Fig. 4. DO removal from SWRO permeate via large membrane systems.

Table 6
Some recent pipeline projects in Chile and Peru

| Plant | Application | ID coating/liner | Location | | Major owner(s) | Startup year | ID, inches | SWRO, L/s | Nominal, ft/s |
|---|---|---|---|---|---|---|---|---|---|
| Candelaria | SWRO | FBE | Punta Padrones | Chile | Lundin Mining Corporation | 2013 | 24 | 500 | 5.6 |
| Collahuasi | Brine | HDPE | Andean Plateau | Chile | Anglo American PLC and Glencore PLC | 2011 | 26 | | |
| Constancia | Tailings | HDPE | Chumbivilcas Province | Peru | Hudbay Minerals Inc. | 2015 | 32 | | |
| Escondida | SWRO | | Puerto Coloso | Chile | BHP Billiton | 2006 | 24 | 525 | 5.9 |
| Escondida | SWRO | Lined [56] | Puerto Coloso | Chile | BHP Billiton | 2018 | 2 × 42 | 2,500 | 4.6 |
| Monturaqui | Aquifer | FBE | Monturaqui | Chile | BHP Billiton | 2017 | 36 and 42 | | |

provides critical redundancy for maintenance and maximum uptime for the largest copper mine in the world [55].

Previously used coatings, for seawater applications or SWRO permeate pipelines, have been cement, polyethylene (PE), polyurethane (PU), FBE, liquid epoxy, coal tar epoxy (external), and glass flake epoxy (internal) [57].

The Collahuasi mine uses a relatively thick high-density polyethylene (HDPE) impulsion, tight fit liner in their 660 mm (26 inches) brine well water pipeline [58]. The liner was installed by using radial compression by passing it through a series of roller reduction units during the insertion process. The liner provides corrosion and abrasion resistance for the C-steel and can be installed with pull lengths up to 1,500 m [58]. Once installed, the liner expands and provides a tight fit. The Hudbay Constantia 813 mm (32 inches) diameter tailings pipeline in Peru uses a very thick-walled HDPE linear [59]. Both Candelaria and Monturaqui [52] used FBE for the internal coating of these water pipelines.

FBE is a thermoset coating that is usually applied at 180°C–250°C in a fluid bed at a thickness of 300–1,000 μm (11.8–39.4 mils) [60], and once properly applied, it is difficult to remove. The FBE coating company should be consulted in terms of the appropriate coating thickness and FBE type per the project details. In the past in Chile, companies were concerned about the coating coming off the pipeline [8], but that was probably due to improper pipe preparation. FBE coatings should be applied per ISO 21809-2 & 3. The pipe should be cleaned of any oil and grease, abrasively cleaned ("sand-blasted") to a Sa-3 near white metal finish, a primer applied and cured, then FBE applied and cured. Finally, the entire coated surface should be a holiday (continuity) tested per ASTM G62 and other standards and repaired (if necessary). Holiday testing is normally used on 20 mils (508 μm) or thinner coatings at 100 V DC or less with a wet sponge and is considered non-destructive. A high voltage spark test (900 to 20,000 V DC) is used on thicker coatings and is considered destructive in that it will attack thin coatings. Note that primers might not be able to be used in drinking water applications per NSF®/ANSI/CAN 61.

Liquid epoxy/PU, on the other hand, is usually applied at 15 mils (381 μm) for inside pipeline coatings, and at 20 mils (508 μm) for liquid epoxy that is NSF®/ANSI/CAN 61 approved for drinking water. In the epoxy/PU formulation, "*the urethane polymer is pre-bonded to the epoxy resin, rendering the coating 'isocyanate free'. The synergistic effect of co-polymerizing epoxy and PU produces a coating with the superior adhesion and corrosion resistance of epoxy along with the added toughness and abrasion resistance of PU.*" [61]. The extra 33% epoxy thickness for drinking water needs to be considered in the planning stages of the project. For protection for the outside of the pipeline, only 5 mils (127 μm) of epoxy thickness is normally required and it is recommended that Zn be added to either PU or liquid epoxy for cathodic protection [60]. Long C-steel pipelines normally need to be cathodically protected.

According to the R&D Center for the Saline Water Conversion Corporation, pipeline coating only represents approximately 5% of the total pipeline cost [62]. In the Chilean example, the average cost was 4.6% (2.6%–8.4% with wall thickness) of the total pipeline cost [50]. But when the cost is a percentage of the pipe, it becomes a function of the pipe diameter, wall thickness, and tensile strength of the C-steel. On a surface area basis, according to Sherwin-Williams, liquid epoxy costs approximately \$43–65/m$^2$ (\$4–6/ft$^2$) in the shop, and \$65–108/m$^2$ (\$6–10/ft$^2$) in the field; while FBE costs approximately \$108–161/m$^2$ (\$10–15/ft$^2$) [63]. Of course all coating costs are obviously a function of the coating thickness. Therefore, the key question is to determine which coating type and thickness will guarantee the desired lifetime of the pipeline [62].

In a detailed experimental study in Saudi Arabia, FBE, two PUs, and a 3-layer PE were evaluated for adhesion after autoclaving at 40°C under a pressure of 103 bar (1,500 psi) with additional flexibility, cathodic disbondment, and salt fog tests. The results showed that the particular FBE chosen was superior to the other coating formulations [62]. There are several acceptable FBE coating variations, from the experiences in the oil and gas industry, and some Chilean SWRO permeate pipelines that should be further investigated for additional lessons learned.

### *7.3. Pipeline installation*

#### *7.3.1. Welding vs. Victaulic® couplings*

To avoid in-the-field grinding of welds, non-destructive weld testing, coating the welds, and holiday testing the coating, a much faster, less-labor intensive, safer and more economical solution is to use Victaulic® grooved mechanical couplings. The pipe ends can be pre-formed in the shop, before coating, to accommodate the Victaulic coupling, and eliminate the risks of coating damage associated with field re-coating internal linings. These risks include improper grinding and surface preparation resulting in poor coating adhesion, putting the welds at risk of corrosion. Additionally, shavings, grindings, slag and sparks from in situ welding and grinding, can damage internal linings, particularly when installing pipe in an uneven terrain, such as the mountainous areas of northern Chile and southern Peru, where these pipelines are often constructed.

In terms of direct installation man-hours, Victaulic grooved mechanical couplings can decrease the field installation time vs. welds by a factor of 5.5 times on average for 102 to 610 mm (4 to 24 inches) diameter pipe as shown in Fig. 5 [64]. Grooved pipe joining can be utilized up to 2,743 mm (108 inches) diameter, and field installation labor savings grow exponentially as diameter increases. Clearly, welding time is directly related to the pipe outside circumference and wall thickness. But there are many other variables that effect welding man-hours such as alloy type, fill angle, electrode diameter, fill rate, rework and field efficiency related to welder skill, jobsite conditions, elevation, etc. Therefore, Fig. 5 should be viewed as nominal times for the Mechanical Contractors Association of America weld data. The Victaulic installation time includes time for preparing a groove, material handling, final coupling installation, and joint inspection [64]. For welded joints on coated or lined pipe, additional labor, equipment and time must be factored in for the total installation time for a well finished joint; however, the Victaulic man-hours reflect the total time for a good finished joint, as there is no coating/lining

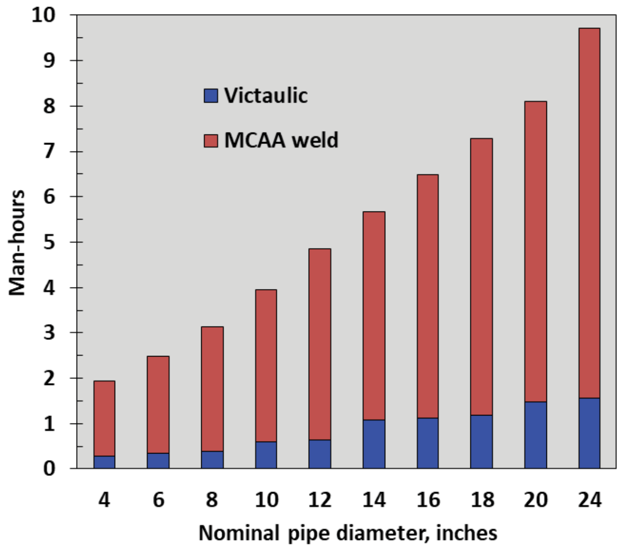


Fig. 5. Victaulic vs. weld installation time, man-hours/joint.

repair, nor any third-party non-destructive inspection such as radiography or liquid dye penetrant.

Victaulic couplings also increase in cut groove and installation time with diameter, as seen in Fig. 5; however, installation is similar for all sizes, keeping installation time stable as diameter increases creating an even more dramatic labor gap when compared to welding. Installation is a relatively simple visual process of lining up the coupling with the groove, aligning the gasket, and properly tightening the hardware. A theoretical 100 km pipeline, with 18 m (60 ft) pipe segments, assuming acceptable terrain, so that shorter pipe sections are not required, would require 5,555 welds. Today there are orbital welders, grinders, and robotic coating equipment with cameras, but welding is still a very time-consuming process, fraught with quality risks at each step.

When considering Victaulic couplings in lieu of welding, in addition to the direct cost savings of labor and material at each joint, one must consider the indirect cost savings related to (1) much smaller crew size, crews of pipefitters (at a lower labor cost) instead of certified welders, (2) the potential to easily assemble above ground with traditional stringing methods or assembling in the ditch with stovepipe construction methods, and (3) the elimination of the need for welding gang crew equipment such as generators, radiography machines, robots, etc. Additionally, couplings can be installed in virtually any site condition, from submarine to arid, hot to cold, windy, or still without the need for tenting, heaters, or other environmental controls. Victaulic couplings are also excellent for the northern Chile and southern Peru seismic zone, which is subject to earthquakes of high intensity [65,66]. Western South America has experienced 5 out of the top 20 earthquakes in the world, with the most powerful one being the Valdivia earthquake in the Biobío region of Chile at 9.5 magnitude.

Victaulic connectors have been applied in earthquake-prone applications and tested in Lehigh University Engineering Research Center's ATLSS Laboratory simulating the 1994 Northridge, CA earthquake with 50% more force (6.85 magnitudes) than the actual 6.7 magnitude earthquake. Testing confirmed the grooved joint's suitability for use in earthquake-prone applications. The Northridge earthquake had estimates of US$20 billion in damage and was the costliest in US history. The peak ground velocity was 1.25 gravity, which was the fastest ever recorded [67]. The coupling allows for movement and the gasket dampens vibrations, which makes it useful for earthquake designs [65].

#### *7.3.2. Rolled vs. cut grooving*

##### *7.3.2.1. Rolled grooving*

In order to attach a Victaulic coupling, the respective pipe needs a proper groove, that is, a cut or rolled groove. Both rolled groove and cut groove pipes will provide the same pressure rating for standard wall pipe. Fig. 6 shows a comparison of rolled groove vs. cut groove piping. Additionally, both rolled and cut grooved pipe can be used in pipelines where intelligent pigs are used for inspection and cleaning.

Rolled grooving, which was developed more than 60 years ago, is used in approximately 90% of grooved piping applications. Rolled grooving is fast, efficient, and a clean pipe-end preparation technique that does not sacrifice pipe performance. Roll grooving for the thickest wall and largest diameter pipe, anticipated in northern Chile and southern Peru, will not take longer than 7 min [68].

It is a cold-forming process that forms a groove on the outside of the pipe as it is compressed and rotated. Today up to 19.1 mm (¾ in) wall thickness can be formed via this technique. Victaulic has designed, manufactures, and supplies the grooving equipment which can conveniently be used at a pipe mill or in the field.

There is no question that a rolled groove causes an indentation inside of the pipe, but testing by Victaulic shows that rolled groove piping contributes only a minor increase in pipeline pressure drop [69]. On tests of 2, 4, 6, and 8-inch (50, 100, 150, and 200 mm) schedule-10 and schedule-40 pipe, the pressure drop increase averaged 4.38% ± 0.98% and was mostly independent of pipe wall thickness and diameter [69]. It should be noted that as pipe diameter increases, the effect of the roll groove indentation on pressure drop greatly decreases.

##### *7.3.2.2. Cut grooving*

Although cut grooving requires more man-hours than rolled grooving, it has the advantage of no pressure drop increase, and as Fig. 5 has shown, requires much less installation time than welding. Cut grooving involves removing a portion of the total pipe wall thickness to provide the groove that the coupling housing engages. Cutting a groove removes less pipe material, to less depth, than pipe threading. Furthermore, although a decrease in wall thickness results in an increase in hoop stress as previously shown in Eq. (6), the coupling housing, which engages the groove, actually reinforces the pipe and prevents diametric expansion [70].

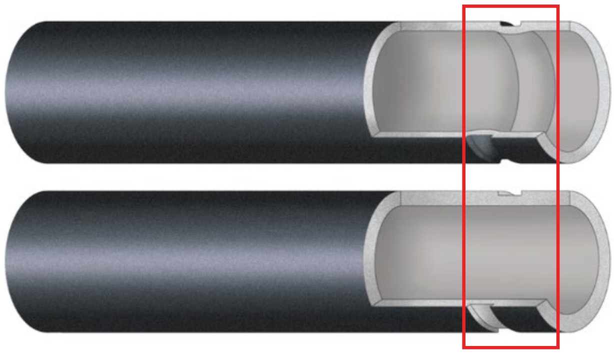

Fig. 6. Rolled groove (top) vs. cut groove piping (courtesy of Victaulic).

This smooth surface allows an easier application of pipe linings and coatings, but there is little or no difference in application time for rolled vs. cut grooves. But the large economic benefit of cut grooving vs. field welding is the huge savings in man-power. Typical cut grooving times are approximately one minute per diameter inch [64].

#### 7.3.3. Pressure performance of couplings

Pressure ratings are identical for both roll and cut grooved standard wall pipe joints and hydrostatic pressure testing results are typically within 5% of each other. Victaulic has tested the fittings to ASTM F-1476 and also there is verification from Underwriters Laboratories, FM approvals, VdS (German), and Landmarks Preservation Commission. The published pressure ratings are established after extensive testing of the ultimate pressure, bending moment, and cyclic loading. In conclusion, grooved mechanical coupling joints are an ideal solution for the long pipelines to serve the mountaintop mines in northern Chile and southern Peru.

## 8. Analysis of using seawater vs. freshwater in the heap leach copper extraction process

Two issues occur when seawater is used for heap leach extraction of copper ores. First, seawater is basic and buffered, so additional acid is required to reduce the water pH to the desired level. Second, the density of seawater impacts the intrinsic permeability of the crushed ore that forms the heap.

### 8.1. Additional acid required to meet the desired pH for the heap leach water

Typical heap leach extraction of copper and other ores uses a solution of water and sulfuric acid with an overall desired pH of 2–3. The use of the unbuffered permeate from a SWRO facility requires a small dose of sulfuric acid to reach the desired pH because the water already has a pH of approximately 5.5–6.5 and no significant concentrations of alkalinity. To reach the equivalent pH using seawater would require >32 times more acid in the heap leaching process. The reason that ">32 times" is used is that SWRO permeate can vary between 100–250 mg/L TDS depending on the seawater salinity, temperature, membrane(s) used and their age, recovery, and flux. Calculations were done from seawater at pH 8.10 to pH 4.30 only, as calculations below the pH range of 4.00–4.30 are not valid, as the Nernst law is not applicable at very low or very high pH values. Nevertheless, this added production cost is very significant because of the requirement to transport the additional acid to the mine site on the mountaintop and the cost of the sulfuric acid itself.

### 8.2. Impact of water density on the crushed ore hydraulic conductivity

Hydraulic conductivity of a porous media is impacted by the density of the fluid moving through it [71]. Assuming that the water temperature is equivalent to using either SWRO permeate or seawater, the primary difference would be restricted to the density ratio between the two water types. Based on the air temperature range on the mountaintop, the water temperature can range from 5°C to 15°C. The SWRO permeate is assumed to have a TDS concentration of 300 mg/L, so the density range would be 999.125 to 1,000.088 mg/kg. The density range for seawater at the same temperature range would be 1,025.653 to 1,027.189 mg/kg. Therefore, the hydraulic conductivity of the heap media would be about 2.7% lower. Therefore, the impact on the heap leach process would be either a slower timeframe for the leaching fluid to move through the crushed ore or the grain size of the heaped crushed ore would have to be increased slightly which would potentially reduce the desired copper yield. The impact is quite difficult to quantify because of the many variables involved and whether more than one metal is being recovered. In addition, the ability to recycle water in the process has greater limitations as evaporative concentration increases the salinity and density of the water which leads to greater declines in hydraulic conductivity.

### 8.3. Impact of water salinity of the recycling potential of the process water

A key issue in mountaintop heap leach extraction of copper is maximizing the use of process water due to the extreme expense of obtaining it. If seawater is used during the process, it has limited recycling potential because of the initial high values of both TDS and sulfate. The use of sulfuric acid in the process combined with the high concentration of sulfate in seawater in addition to high evaporation rates can increase the concentration to a critical value causing precipitation of gypsum or other sulfate minerals within the basal part of the heap. Therefore, one or perhaps two reuse cycles of seawater may be possible. If freshwater (desalted seawater) is used, the potential for recycling is quite high and somewhere between 4 and 7 cycles could be used depending on the local geochemistry of the heap rock material. Therefore, it is estimated that the potential for recycling for freshwater is at least 70% higher than for seawater.

### *8.4. Potential impacts of process water salinity on the operation of the electrode copper concentration process*

The placement of high salinity water into the copper concentration process wherein electrodes are used may be problematic. There is a limit on the conductivity of the water within the system. Therefore, beginning with a seawater salinity, the limit may be exceeded without the ability to recycle the water.

## 9. Analysis of environmental impacts of using seawater in heap leach copper extraction in mountaintop environments

During mountaintop mining and processing of copper, protection of the environment is quite important and has economic importance. Government permits have some specific restrictions governing compliance, particularly with regard to water quality that could affect downstream surface water. Some surface water basins have headwaters near mining sites in Chile and Peru. Therefore, the minimization of waste products is important. The use of seawater accelerates the generation of waste brines and bulk salt. This necessitates the development of onsite infrastructure to store or dispose of this salt in a manner that isolates it from downstream surface waters. Fortunately, most of the areas that require water from the sea are arid and rainfall events are rare, which reduces saline runoff risk generation. There is no reasonable method to value the environmental risk issue in using seawater at the mine sites.

## 10. Discussion

A comparison of the key issues in deciding whether to use SWRO permeate or seawater in heap leach copper extraction is summarized in Table 7. As can be observed, the balance in the various cost factors produces a rather murky picture of which water source truly creates lower copper production cost.

The highest capital and operating cost difference occurred in comparing the pretreatment of seawater to full SWRO desalination wherein the same process train is used for conditioning of the seawater for direct use or pretreatment for SWRO (screening followed by UF). The cost of pretreatment has been documented to show that using DAF/UF as pretreatment is about 30% of the total cost for desalination of seawater [72]. In both cases, a coated or lined transmission pipe is required if the pH of permeate is maintained from the plant to the mountaintop. Even if post-treatment of permeate is added along with a corrosion inhibitor, a coated pipe may still be required and then, the added use of acid would become problematic. The issue of the 6.5% greater horsepower required for pumping of the seawater could add the capital cost of an additional pumping station depending on the distance and elevation differential. Two key balancing cost factors favoring the use of SWRO permeate is the ability to reuse the water through several cycles of heap leach extraction before the ionic strength of the water becomes too great and a reduced volume of sulfuric acid required. The use of seawater may allow only one reuse cycle before the impact of the density on the hydraulic conductivity of the crushed rock in the heap becomes problematic. If the density (salinity) is too high then the grain size of the heap material would have to be increased to increase the hydraulic conductivity, which could reduce copper yield caused by a reduction in surface area. Based strictly on the combined capital and operating costs, the use of SWRO permeate or seawater is close.

Perhaps the two issues that could swing the balance in favor of using the SWRO permeate are the socio-political and environmental issues. During the permitting process, the ability to offer some freshwater to local residents near the coast, along the pathway to the mine, could be greatly beneficial. The future use of the SWRO facility beyond the lifetime of the mine could be an additional benefit. This could involve a transfer of ownership to the regional government or a sale of the facility. An important environmental issue is the disposal of the residual water (brine) and/or salt from the copper extraction process. The use of seawater would increase the overall volume of the combined brine and salt, especially when considering the >32 times additional volume of sulfuric acid required to obtain the proper heap leaching pH. Since some mines are at the top of stream drainage basins, the downward movement

Table 7
Qualitative comparison of issues of SWRO permeate vs. partially-treated seawater

| Issue | SWRO permeate | Partially-treated seawater |
|---|---|---|
| Treatment cost | +70% | – |
| Pump efficiency | – | –6.5% |
| Pumping stations required | – | +1? |
| Transmission pipe corrosion | Coated or lined pipe required | Coated or lined pipe required |
| Sulfuric acid used in process | – | >32 times |
| Hydraulic conductivity of the heap media | – | –2.7% |
| Water reuse potential | – | Up to 70% lower |
| Impacts on electrode copper extraction process | – | Negative |
| Environmental issues | – | Greater |
| Socio-political | Positive | Negative |

of brine could be problematic. This may not be the case in hyperarid areas, but the residential brine salt will still require temporary disposal during the operation and ultimately permanent disposal.

## 11. Conclusions

Copper mining and onsite processing in arid regions require water, particularly in the heap leach extraction process. Only two sources of water are available in many regions, such as southern Peru and northern Chile, which are partially-treated seawater and desalinated seawater (freshwater). The choice concerning which water type to use is complex in consideration that the water must be transported 10–200 km and at elevations between 600 and 4,900 m above sea level. In addition, the water type used impacts the efficiency of the heap leach copper extraction process.

After extensive analysis, it is concluded that the overall cost of using partially-treated seawater or desalted seawater is essentially equivalent when considering all factors including, treatment, transport, and impacts on the heap leach process. The cost of treatment is higher for the desalination of seawater (70% greater). The cost of pumping the denser seawater is greater because the pump efficiency is 6.5% lower. In both cases, the epoxy-coated transmission pipe should be used. Seawater used in the heap leach process requires greater than 32 times more sulfuric acid to meet the desired average pH of about 2.5 and has a reduced hydraulic conductivity of 2.6% when passing through the porous media of the crushed rock. In addition, the reuse of the process water has a much lower potential when using seawater, which can increase the actual amount of water that must be pumped up the mountain. The use of seawater requires greater disposal of residuals and has potential environmental issues. The desalination facility may have a greater life expectancy compared to the mine and could have significant residual value. The potential environmental issues and the residual value of the plant tend to cause the use of freshwater (desalted seawater) to be the preferred water source in consideration of the socio-political support of copper mines at most sites.

## Acknowledgments

The authors thank Mr. Jerry Rowe for providing some fundamental information on the copper heap leach process. Funding for the research was from the Emergent Technologies Institute, U.A. Whitaker College of Engineering, Florida Gulf Coast University.

## References

[1] R.G. Krauth, Controlled Percolation System and Method for Heap Leach Mining, The United States Patent 5,005,806, April 9, 1991.
[2] S.C. Bouffard, D.G. Dixon, Investigative study into the hydrodynamics of heap leaching processes, Metall. Mater. Trans. B, 32 (2001) 763–776.
[3] M.E. Schlesinger, M.J. King, K.C. Sole, W.G. Davenport, Extractive Metallurgy of Copper, 5th ed., Elsevier, The Netherlands, 2011.
[4] A. Guzmán-Guzmán, O.Y. Cáceres Hernández, R. Srivastava, J.W. Jones, Integrated Process Control to Enhance Heap Leach Performance, Proceedings of the Second International Conference on Heap Leach Solutions, Peru, June 25, 2014.
[5] S. Thomashausen, K. Hamil, Water Risks in the Mining Sector, Chile, Columbia Center on Sustainable Investment, A Joint Center of Columbia Law School, and the Earth Institute, Columbia University, New York, August 2016. Available at: http://ccsi.columbia.edu/files/2016/06/Water-Template-Chile.pdf.
[6] L. Banchik, Chile's Thirst for Water: A Chilean City Famous for Mining in the Atacama Desert is Running Out of Water. Fast., Available at: http://latinamericanscience.org/2014/05/chiles-thirst-for-water/ (accessed 20 September 2019).
[7] L.A. Cisternas, E.D. Gálvez, The use of seawater in mining, Miner. Process. Extr. Metall. Rev., Int. J., 39 (2018) 18–33.
[8] S. González, M.T. Ramírez, R. Muñoz, J. Zúñiga, The Impact of Corrosion on Mine Water Supply Systems, Water in Mining 2012, Proceedings of the 3rd International Congress on Water Management in the Mining Industry, Santiago, June 6–8, 2012.
[9] F. Els, The World's 10 Highest Mines, Mining.com, Glacier RIG (Resource Innovation Group) Ltd., Vancouver, BC, Canada, Dec. 16, 2015. Available at: https://www.mining.com/the-worlds-10-highest-mines/ (accessed December 2019).
[10] R.P. Genereaux, Fluid-flow design methods, Ind. Eng. Chem., 29 (1937) 385–388.
[11] M.S. Peters, K.D. Timmerhaus, Plant Design and Economics for Chemical Engineers, 2nd ed., McGraw-Hill Book Company, New York, 1968, pp. 302–308.
[12] M.S. Peters, K.D. Timmerhaus, Plant Design and Economics for Chemical Engineers, 3rd ed., McGraw-Hill Book Company, New York, 1980, pp. 377–383.
[13] M.S. Peters, K.D. Timmerhaus, Plant Design and Economics for Chemical Engineers, 4th ed., McGraw-Hill Book Company, New York, 1991.
[14] C.B. Nolte, Optimum Pipe Size Selection, 1st ed., Trans Tech Publications, 1978.
[15] W. Saeed, Chemical Engineering Projects, Design and Calculation of Chemical Engineering Projects, Pipe Size Selection, Karachi, Pakistan, April 28, 2014. Available at: https://chemicalprojects.wordpress.com/2014/04/28/pipe-size-selection/ (accessed September 15, 2019).
[16] R.W. Whitesides, Selecting the Optimum Pipe Size, PDH online Course M270 (12 PDH), Fairfax, VA, 2015. Available at: https://www.pdhonline.com/courses/m270/m270content.pdf (accessed May 20, 2019).
[17] W. Copan, National Institute of Standards and Technology (NIST), Standard Acceleration of Gravity, US Department of Congress, Gaithersburg, MD, 2019. Available at: https://physics.nist.gov/cgi-bin/cuu/Value?gn (accessed on May 20, 2019).
[18] P.R.H. Blasius, Das Aehnlichkeitsgesetz bei Reibungsvorgangen in Flüssigkeiten. Forschungsheft, 1913, pp. 131:1–41.
[19] K.T. Trinh, On the Blasius Correlation for Friction Factors, Institute of Food Nutrition and Human Health, Massey University, New Zealand, July 2010.
[20] C.M. Burt, X.S. Piao, F. Gaudi, B. Busch, N.F.N. Taufik, Electric motor efficiency under variable frequencies and loads, J. Irrig. Drain. Eng., 134 (2008).
[21] USDOE, Buying an Energy-Efficient Electric Motor, Fact Sheet, U.S. Department of Energy, 2014. Available at: https://www.energy.gov/sites/prod/files/2014/04/f15/mc-0382.pdf. (accessed November 15, 2019).
[22] American National Standard for Rotodynamic Pumps – Guideline for Effects of Liquid Viscosity on Performance, ANSI/HI Guideline 9.6.7, Hydraulics Institute, New Jersey, 2015.
[23] Sea Temperature Organization, Monthly Taltal Water Temperature Chart, World Sea Temperatures with Ezoic Inc., Carlsbad, CA, 2019. Available at: https://www.seatemperature.org/south-america/chile/taltal-march.htm (accessed on September 20, 2019).
[24] J. Honeywell, Effect of Viscosity on Pump Performance, PetroSkills, 2006. Available at: http://www.jmcampbell.com/tip-of-the-month/2006/08/effect-of-viscosity-on-pump-performance/ (accessed on April 20, 2019).

[25] Price List of Carbon Steel Pipes & Tubes, Seamless Pipe, Welded Pipe, Reliable Pipes & Tubes Ltd., 2019. Available at: https://www.reliablepipestubes.com/blog/price-pricelist-carbon-steel-pipe-seamless-pipe-welded-pipe/ (accessed on July 30, 2019).
[26] A.A. Durand, M.J. de Villafranca Casas, A.S.G. Cornejo, D.J. Carranza, F.J.P. Román, R.G.S. Suárez, J.S. Espinoza, L.F. Villalobos, V. de la Parra, Updating the rules for pipe sizing, Chem. Eng., 117 (2010) 48–50.
[27] NOAA's Adopt A Drifter Program, Ocean Currents Map, 2019. Available at: https://www.adp.noaa.gov/OceanCurrentsMap.aspx.
[28] C. Wisskirchen, J. Waples, F. Vásquez, Considerations for Seawater in Mining: Approaches to Evaluate ARD and Metals Leaching Potential, Water in Mining 2012, Proceedings of the 3rd International Congress on Water Management in the Mining Industry, Santiago, Chile, June 6–8, 2012.
[29] IOC, SCOR, IAPSO, The International Thermodynamic Equation of Seawater – 2010: Calculation and Use of Thermodynamic Properties, Intergovernmental Oceanographic Commission, Manuals and Guides No. 56, UNESCO (English), 2010, 196p.
[30] T. Pankratz, Water Desalination Report, Global Water Intelligence, Media Analytics, Oxford, UK, 2019.
[31] A.U. Malik, I.N. Andijani, M. Mobin, S. Ahmad, Corrosion behavior of materials in RO water containing 250–350 ppm chloride, Desalination, 196 (2006) 149–159.
[32] USGS, Dissolved Oxygen Solubility Tables, U.S. Geological Survey, Aug 8, 2018. Available at: https://water.usgs.gov/software/DOTABLES/ (accessed August 10, 2019).
[33] A.H.A. Dehwah, H. Cheng, T.M. Missimer, P.-Y. Hong, Understanding microbial assembly on seawater reverse osmosis membranes to facilitate evaluation of seawater pretreatment options, Desal. Water Treat., 170 (2019) 1–10.
[34] B.O. Hasan, Effect of salt content on the corrosion rate of steel pipe in turbulently flowing solutions, Al-Nahrain Univ., Coll. Eng. J. (NUCEJ), 13 (2010) 66–73.
[35] M. Yari, An Intro to Pipeline Corrosion in Seawater, Edmonton, AL Canada, 2017. Available at: https://www.corrosionpedia.com/2/1432/corrosion-101/an-intro-to-pipeline-corrosion-in-seawater (accessed on August 20, 2019).
[36] N.A.A. Alameer, The Effect of Temperature and pH on the Corrosion Rate of Carbon Steel in 1 M NaCl, Technical College, Bagdad, Iraq, 2010. Available at: https://www.iasj.net/iasj?func=fulltext&aId=29410.
[37] NACE International, Corrosion Control and Monitoring in Seawater Injection Systems, Houston, TX, NACE SPO499–2007.
[38] J. Carew, A. Al-Hashem, E.A. Al-Mohemeed, H.Y. Al-Anzi, Intelligent pigging of a seawater injection pipeline in Kuwait, Mater. Perform., 48 (2009) 44–47.
[39] Fluor® Projects, Atacama Natural Gas Pipeline, Fluor Corporation, Irving, TX, 2019. Available at: https://www.fluor.com/projects/onshore-natural-gas-pipeline-epcm (accessed December 18, 2019).
[40] X. Wang, R.E. Melchers, Long-term under-deposit pitting corrosion of carbon steel pipes, Ocean Eng., 133 (2017) 231–243.
[41] NOAA (National Oceanic and Atmospheric Administration), Science on a Sphere®, National Oceanic and Atmospheric Administration, Ocean Acidification: Surface pH, US Department of Congress, Washington, DC, 2019. Available at: https://sos.noaa.gov/datasets/ocean-acidification-surface-ph/.
[42] J.F. Waters, Measurement of Seawater pH: A Theoretical and Analytical Investigation, Doctor of Philosophy Dissertation, University of Miami, Florida, 2012.
[43] Climate Change 2013, The Physical Science Basis, Summary for Policymakers, Technical Summary and Frequently Asked Questions, Part of the Working Group I Contribution to the Fifth Assessment Report of the Intergovernmental Panel on Climate Change, Cambridge University Press, Cambridge, UK, 2013, p. 28.
[44] J.C. Orr, V.J. Fabry, O. Aumont, L. Bopp, S.C. Doney, Anthropogenic ocean acidification over the twenty-first century and its impact on calcifying organisms, Nature, 437 (2005) 618–686.
[45] A.H.A. Dehwah, T.M. Missimer, Subsurface intake systems: green choice for improving feed water quality at SWRO desalination plants, Jeddah, Saudi Arabia, Water Res., 88 (2016) 218–224.
[46] D.M. Anderson, Toxic Algal Blooms and Red Tides: A Global Perspective, T. Okaichi, D.M. Anderson, T. Nemoto, Eds., Red Tides: Biology, Environmental Science and Toxicology, The Netherlands, Elsevier, 1989, pp. 11–16.
[47] G. Dvorsky, Sigma Xi SmartBrief, Stunning but Deadly, China's Bioluminescent Algal Blooms are Getting Bigger, Gizmodo.com owned by Great Hill Partners, Boston, MA, 2019. Available at: https://gizmodo.com/stunning-but-deadly-china-s-bioluminescent-algal-bloom-1835482191 (accessed on December 6, 2019).
[48] D.M. Anderson, S.F.E. Boerlage, M.B. Dixon, Harmful Algal Blooms (HABs) and Desalination: A Guide to Impacts, Monitoring, and Management, Paris, Intergovernmental Oceanographic Commission of UNESCO, (IOC Manuals and Guides No. 78) (English) (IOC/2017/MG/78), United Nations Educational, Scientific and Cultural Organization, Paris, France, 2017, 538 p.
[49] NACE International, Internal Corrosion for Pipelines – Advanced Course Manual, Houston, TX, Sept 2009.
[50] S. González, M. Encalada, S. Daughney, T. Vece, Selection of Pipeline Corrosion Control Strategy and Impact on Economics of Water Conveyance, Water in Mining 2010, Proceedings of the 2nd International Congress on Water Management in the Mining Industry, Santiago, Chile, June 9–11, 2010.
[51] A. Ismail, N.H. Adan, Effect of oxygen concentration on corrosion rate of carbon steel in seawater, Am. J. Eng. Res. (AJER), 3 (2014) 64–67.
[52] Aegion® Coating Services, St. Louis, MO, 2019. Available at: https://www.aegion.com/about/resources/case-studies/escondida-slurry-pipe-coating.
[53] Lundin Mining, Technical Report for the Candelaria Copper Mining Complex, Atacama Region, Region III, SRK Consulting, Chile, 2018.
[54] Escondida, BHP opens Escondida Water Supply, the Largest Desalination Plant in Latin America, International Mining, 2018. Available at: https://im-mining.com/2018/04/07/bhp-opens-escondida-water-supply-largest-desalination-plant-latin-america/ (accessed December 6, 2019).
[55] Mining for Zambia, A Zambia Chamber of Mines Initiative, The World's Biggest Copper Mines, Industry Wide Website for Mining in Zambia, Zambia, Africa, 2019. Available at: https://miningforzambia.com/worlds-biggest-copper-mines/ (accessed on May 20, 2019).
[56] Bechtel, Delivering a Reliable, Sustainable Water Supply, Bechtel Corporation, San Francisco, CA, 2019. Available at: https://www.bechtel.com/projects/escondida-water-supply/.
[57] C. Smith, T. Siewert, B. Mishra, D. Olson, A. Lassiegne, Eds., Coatings for Corrosion Protection: Offshore Oil and Gas Operation Facilities, Marine Pipeline and Ship Structure, NIST Special Publication 1035, United States Department of Transportation, Biloxi, Mississippi, April 14–16, 2004.
[58] Allied Pipeline Technologies, Collahuasi – Impulsion Water Line Coating with Sure-Liner™ HDPE, Durango, CO, 2019. Available at: https://alliedpipelinetechnologies.com/collahuasi (accessed October 12, 2019).
[59] Allied Pipeline Technologies, Peru Hudbay Constancia Tailings Pipeline, Durango, CO, 2019. Available at: https://alliedpipelinetechnologies.com/peru-hudbay (accessed December 19, 2019).
[60] Keith Industries, Fusion Bonded Epoxy (FBE), Rosharon, TX, 2019. Available at: https://keithinc.com/index.php/fusion-bond-epoxy-fbe/ (accessed May 20, 2019).
[61] Specialty Polymer Coatings (SPC), Products. Epoxy, Langley, BC, Canada, 2019. Available at: http://www.spc-net.com/products/?cat=Type&val=epoxy (accessed November 15, 2019).
[62] A.U. Malik, S. Ahmad, I. Andijani, F. Al-Muaili, T.L Prakash, J. O'Hara, Corrosion Protection Evaluation of Some Organic Coatings in Water Transmission Lines, Saline Water Conversion Corporation, Technical Report, No. TR 3804/APP 95009, Al-Jubail, Kingdom of Saudi Arabia, 1999.
[63] J. Hair, Y. Idlibi, Sherwin-Williams Liquid Epoxy Coatings Offer Cost Effective Alternative, The Sherwin-Williams Company,

Inc., Cleveland, OH, 2010. Available at: https://www.hartenergy.com/news/sherwin-williams-liquid-epoxy-coatings-offer-cost-effective-alternative-52270.

[64] J.R. Renner, Communication, Vice President, Victaulic Company, Easton, PA, November 21, 2019.

[65] Victaulic®, Design Data for Seismic Applications of Victaulic Grooved System, 26.12, Easton, PA, 2010.

[66] USGS, 20 Largest Earthquakes in the World, U.S. Geological Survey, 2019. Available at: https://www.usgs.gov/natural-hazards/earthquake-hazards/science/20-largest-earthquakes-world?qt-science_center_objects=0#qt-science_center_objects (accessed August 10, 2019).

[67] California Department of Conservation, Sacramento, CA, 2019. Available at: https://www.conservation.ca.gov/cgs/earthquakes/northridge.

[68] W. Biery, Communication, Director – Large Diameter Systems and Hydrotransport, Victaulic Company, Easton, PA, November 21, 2019.

[69] Victaulic®, Style HP-70 Rigid High Pressure Coupling, Manual VS103.1, Easton, PA, 2017. Available at: https://www.victaulic.com/products/style-hp-70-rigid-high-pressure-coupling/ (accessed August 15, 2019).

[70] G. Trinker, Common Myths About Mechanical Pipe Joints, in the Groove; PutmanMedia®, Schaumburg, IL, 2010. Available at: https://www.plantservices.com/articles/2010/04 MechanicalPipeJoints/ (accessed on November 15, 2019).

[71] C.W. Fetter, Applied Hydrogeology, 4th ed., Prentice Hall, New Jersey, 2001.

[72] T.M. Missimer, N. Ghaffour, A.H.A. Dehwah, R. Rachman, R.G. Maliva, G.L. Amy, 2013, Subsurface intakes for seawater reverse osmosis facilities: capacity limitation, water quality improvement, and economics, Desalination, 322 (2013) 37–51.